Title

Airborne observations of methane emissions from rice cultivation in the Sacramento Valley of California

Journal

Journal of Geophysical Research Atmospheres, 117(23)

ISSN

0148-0227

Authors

Peischl, J
Ryerson, TB
Holloway, JS
et al.

Publication Date

2012

DOI

10.1029/2012JD017994

Airborne observations of methane emissions from rice cultivation in the Sacramento Valley of California

J. Peischl,[1,2] T. B. Ryerson,[2] J. S. Holloway,[1,2] M. Trainer,[2] A. E. Andrews,[3] E. L. Atlas,[4] D. R. Blake,[5] B. C. Daube,[6] E. J. Dlugokencky,[3] M. L. Fischer,[7] A. H. Goldstein,[8] A. Guha,[8] T. Karl,[9] J. Kofler,[1,3] E. Kosciuch,[1,2] P. K. Misztal,[8,9] A. E. Perring,[1,2] I. B. Pollack,[1,2] G. W. Santoni,[6] J. P. Schwarz,[1,2] J. R. Spackman,[1,2] S. C. Wofsy,[6] and D. D. Parrish[2]

Received 24 April 2012; revised 12 August 2012; accepted 7 October 2012; published 8 December 2012.

[1] Airborne measurements of methane (CH_4) and carbon dioxide (CO_2) were taken over the rice growing region of California's Sacramento Valley in the late spring of 2010 and 2011. From these and ancillary measurements, we show that CH_4 mixing ratios were higher in the planetary boundary layer above the Sacramento Valley during the rice growing season than they were before it, which we attribute to emissions from rice paddies. We derive daytime emission fluxes of CH_4 between 0.6 and 2.0% of the CO_2 taken up by photosynthesis on a per carbon, or mole to mole, basis. We also use a mixing model to determine an average CH_4/CO_2 flux ratio of −0.6% for one day early in the growing season of 2010. We conclude the CH_4/CO_2 flux ratio estimates from a single rice field in a previous study are representative of rice fields in the Sacramento Valley. If generally true, the California Air Resources Board (CARB) greenhouse gas inventory emission rate of 2.7×10^{10} g CH_4/yr is approximately three times lower than the range of probable CH_4 emissions ($7.8–9.3 \times 10^{10}$ g CH_4/yr) from rice cultivation derived in this study. We attribute this difference to decreased burning of the residual rice crop since 1991, which leads to an increase in CH_4 emissions from rice paddies in succeeding years, but which is not accounted for in the CARB inventory.

Citation: Peischl, J., et al. (2012), Airborne observations of methane emissions from rice cultivation in the Sacramento Valley of California, *J. Geophys. Res.*, *117*, D00V25, doi:10.1029/2012JD017994.

1. Introduction

[2] Methane (CH_4) is a potent greenhouse gas whose emissions in California are regulated under Assembly Bill 32, signed into law as the Global Warming Solutions Act of 2006, which requires statewide greenhouse gas emissions not to exceed 1990 levels by the year 2020. Effective regulation requires accurate knowledge of the distribution and relative contributions of CH_4 sources within California, which include livestock, landfills, wastewater treatment, oil and gas drilling and distribution, and rice cultivation. An inventory of annually averaged greenhouse gas emissions for California was developed by the California Air Resources Board (CARB) in order to quantify these emissions.

[3] In CARB's CH_4 inventory, rice cultivation accounts for approximately 1.8% of California's annually averaged anthropogenic CH_4 emissions (http://www.arb.ca.gov/cc/inventory/data/data.htm, accessed August 2012). However, the majority of these rice emissions occurs during the growing season, which typically runs from mid-May to the end of August [*McMillan et al.*, 2007]. Therefore, during the growing season, rice cultivation should account for approximately 6–7% of California's anthropogenic methane emissions, which is similar in magnitude to the emissions from oil and gas extraction (approximately

[1]Cooperative Institute for Research in Environmental Sciences, University of Colorado Boulder, Boulder, Colorado, USA.
[2]Earth System Research Laboratory, Chemical Sciences Division, National Oceanic and Atmospheric Administration, Boulder, Colorado, USA.
[3]Earth System Research Laboratory, Global Monitoring Division, National Oceanic and Atmospheric Administration, Boulder, Colorado, USA.
Corresponding author: J. Peischl, Earth System Research Laboratory, Chemical Sciences Division, National Oceanic and Atmospheric Administration, 325 Broadway, R/CSD7, Boulder, CO 80305, USA. (jeff.peischl@noaa.gov)

0148-0227/12/2012JD017994

[4]Rosentstiel School of Marine and Atmospheric Science, Division of Marine and Atmospheric Chemistry, University of Miami, Miami, Florida, USA.
[5]Department of Chemistry, University of California, Irvine, California, USA.
[6]Department of Earth and Planetary Sciences, School of Engineering and Applied Science, Harvard University, Cambridge, Massachusetts, USA.
[7]Lawrence Berkeley National Laboratory, Energy and Environmental Technologies Division, Berkeley, California, USA.
[8]Department of Environmental Science, Policy, and Management, University of California, Berkeley, California, USA.
[9]Atmospheric Chemistry Division, National Center for Atmospheric Research, Boulder, Colorado, USA.

8%), making it one of the larger non-livestock methane emission sectors during this time of year.

[4] Several previous works have examined CH_4 fluxes from California rice paddies [e.g., *Cicerone et al.*, 1992; *Lauren et al.*, 1994; *Bossio et al.*, 1999; *Fitzgerald et al.*, 2000; *Redeker et al.*, 2000; *McMillan et al.*, 2007]. Here we focus on the work of *McMillan et al.* [2007] because they additionally measured carbon dioxide (CO_2) fluxes, which, in combination with CH_4 fluxes, provide a more complete greenhouse gas picture and a basis for a flux ratio comparison. *McMillan et al.* [2007] measured fluxes at one rice paddy (39.28°N latitude, 122.18°W longitude) located in the Sacramento Valley of California. This was a multiyear project that included three growing seasons from 2000 to 2002. They showed that during the growing season, CH_4 and CO_2 emissions were negatively correlated during the daytime (i.e., CH_4 was emitted while CO_2 was taken up by the rice crop during photosynthesis), and positively correlated at nighttime (i.e., CH_4 was emitted while CO_2 was respired). They determined stoichiometric flux ratios of CH_4 to CO_2 throughout the project. Although CH_4 is produced by microbes in the soil, the main pathway for this CH_4 to reach the atmosphere during the growing season is through the rice plants [*Cicerone and Shetter*, 1981; *Le Mer and Roger*, 2001], while other pathways, such as ebullition and diffusion, are co-located with the rice plants. As a result, correlations of CH_4 emissions with CO_2 uptake reported by *McMillan et al.* [2007] are high ($r^2 > 0.98$), and it is this signal, once vertical mixing has occurred, that we determine from samples taken aboard an instrumented research aircraft. Specific to the analysis below, *McMillan et al.* [2007] determined daytime CH_4/CO_2 flux ratios of −0.6% (per carbon, or mole to mole) during the seedling stage (0–23 days after planting) and −2.7% during the mid-vegetative stage (24–47 days after planting) of rice growth. However, that study was necessarily confined to one rice paddy and dependent on the farming practices of one rice farmer. This paper complements the work of *McMillan et al.* [2007] by expanding the spatial domain to the entire rice growing region of the Sacramento River Valley for three days: two in the Spring of 2010 and one in the Spring of 2011.

[5] We use data from two flights of a chemically instrumented National Oceanic and Atmospheric Administration (NOAA) P-3 research aircraft over the rice-growing region of the Sacramento Valley, where the majority of rice paddies in California are located (e.g., see http://www.nass.usda.gov/Charts_and_Maps/Crops_County/ar-ha.asp), to examine the possible sources of CH_4 emissions during the flights. The two flights occurred on 11 May (before the growing season) and 14 June (during the growing season) 2010, during the California Research at the Nexus of Air Quality and Climate Change (CalNex) field study. For the 14 June flight, we use ancillary measurements of black carbon (BC) to separate biomass burning emissions of CH_4 and CO_2 from the expected emissions of CH_4 and uptake of CO_2 from the rice paddies. We also use correlations with carbon monoxide (CO) to discriminate between urban and rice paddy emissions of CH_4. Next, we show that CH_4 and CO_2 data over rice paddies are consistent with the findings of *McMillan et al.* [2007], and use a mathematical model to determine that the ratios of CH_4 and CO_2 fluxes measured by *McMillan et al.* [2007] from one rice paddy in 2000–2002 are representative of an area-wide survey of the majority of California's rice paddies for one day in 2010.

[6] Additionally, we use data from a flight of an instrumented Center for Interdisciplinary Remotely Piloted Aircraft Studies (CIRPAS) Twin Otter on 15 June 2011, during the California Airborne Biogenic Volatile Organic Compound Emission Research in Natural Ecosystem Transects (CABERNET) field campaign, which support the CH_4/CO_2 flux ratio determined by measurements from the NOAA P-3 in 2010 and the work of *McMillan et al.* [2007].

2. Instrumentation

2.1. CO_2 and CH_4 Instrumentation and Description

[7] CO_2 and CH_4 were measured aboard both aircraft using a modified commercial wavelength-scanned cavity ring-down analyzer (Picarro 1301-m) [*Crosson*, 2008]. Though sold as a $CO_2/CH_4/H_2O$ analyzer, we included a drier in the sample flow and did not measure H_2O to increase the sampling frequency for both CO_2 and CH_4 to 1 Hz.

[8] Atmospheric air was sampled through a 0.95 cm (3/8 in.) OD stainless steel rearward facing inlet on the NOAA P-3 and from the main inlet on the CIRPAS Twin Otter [*Hegg et al.*, 2005], and dried to a dew point temperature of −78°C by passage through a 200-strand Nafion dryer (p/n PD-200 T-24MPS) and a dry ice trap [*Peischl et al.*, 2010]. The absorption cell pressure was controlled at 140 Torr (±0.2 Torr during smooth flight, and ±0.5 Torr during typical boundary layer flight conditions; all stated uncertainties are $\pm 1\sigma$). Absorption cell pressure instability led to decreased precision in the turbulent daytime boundary layer, as discussed in more detail below.

[9] Immediately inside the fuselage, two CO_2 and CH_4 calibration gas standards were regularly delivered to the inlet line during flight to evaluate instrument sensitivity. The calibration standards bracketed the expected ambient range of each gas and were known to within ±0.07 ppmv CO_2 and ±1 ppbv CH_4 (all CO_2 and CH_4 mixing ratios are reported as dry air mole fractions). The calibration gases were added at a flow rate sufficient to displace ambient air and overflow the inlet. These flight standard tanks, or secondary standards, were calibrated before and after the field project using primary CO_2/CH_4 standard tanks tied to the WMO standard from the Global Monitoring Division (GMD) at the NOAA Earth System Research Laboratory (ESRL) [*Dlugokencky et al.*, 2005; *Zhao and Tans*, 2006]. A third calibration standard (referred to here as a "target" [*Daube et al.*, 2002; *Peischl et al.*, 2010]) was regularly introduced to the inlet between calibrations and treated as an unknown to evaluate long-term instrument performance (Figure 1). The accuracy of the 20-s averaged target retrievals did not depend on flight conditions, as the pre-flight target retrievals are statistically equal to the in-flight retrievals. Isotopic corrections for ^{13}C and ^{18}O were made to calibration and ambient CO_2 data following the work of *Chen et al.* [2010], and assumptions of isotopic abundance in California air between May and June were based on long-term measurements at Trinidad Head and Pt. Arena, California (J. W. C. White and B. H. Vaughn, Stable Isotopic Composition of Atmospheric Carbon Dioxide (^{13}C and ^{18}O) from the NOAA ESRL Carbon Cycle Cooperative Global Air Sampling Network, 1990–2008, 2009, ftp://ftp.cmdl.noaa.gov/ccg/co2c13/flask/event/).

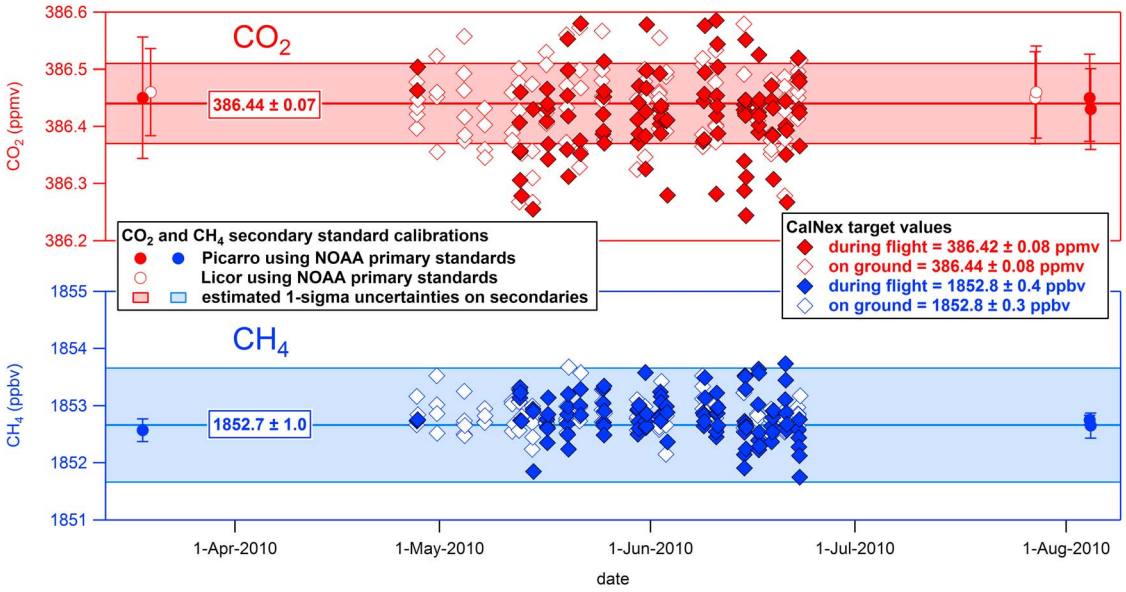

Figure 1. In-flight target retrievals from CalNex data set (red and blue diamonds). Pre-flight target retrievals are included for comparison (white diamonds). Calibrated in the lab with primary standards from NOAA ESRL GMD before and after CalNex, the CO_2 target tank averaged 386.44 ppmv and the CH_4 target tank averaged 1852.7 ppbv, with no significant drift in either. These numbers are represented by the solid horizontal lines in the graphs. In-flight CO_2 target retrievals averaged 386.42 (±0.08) ppmv; pre-flight target retrievals while the aircraft was on the ground averaged 386.44 (±0.08) ppmv. In-flight CH_4 target retrievals averaged 1852.8 (±0.4) ppbv; pre-flight target retrievals averaged 1852.8 (±0.3) ppbv. The $\pm 1\sigma$ limits are represented by the shaded area in the graph. Due to a leak in the calibration system, in-flight calibrations from 30 April–11 May are not included.

To check these isotopic corrections, the flight standard tanks were additionally calibrated for CO_2 with a different set of GMD primary tanks using a modified LI-COR 6262 CO_2 analyzer [*Peischl et al.*, 2010]. These analyses yielded the same calibrated CO_2 mixing ratio value as those performed with the aircraft instrument (Figure 1). The uncertainties of the flight standards, shown as the shaded areas in Figure 1, are dominated by the uncertainties in the primary standards.

[10] Independent of the target retrievals, we estimate a total uncertainty in the measurements by summing in quadrature the known sources of uncertainties. We derive combined inaccuracy in CO_2 of ±0.10 ppmv and in CH_4 of ±1.2 ppbv, with the error attributed to each individual term as follows (given for CO_2, CH_4): primary standard uncertainty (±0.07 ppmv, ±1.0 ppbv), additional secondary standard uncertainty (±0.02 ppmv, ±0.1 ppbv), calibration uncertainty (±0.06 ppmv, ±0.6 ppbv), and isotope correction uncertainty (±0.015 ppmv, negligible). One-second imprecision of the CO_2 measurement was ±0.10 ppmv during smooth flight and ±0.15 ppmv during turbulent flight. One-second imprecision of the CH_4 measurement was ±1.5 ppbv during smooth flight and ±2.0 ppbv during turbulent flight. The estimated uncertainties were similar for the installation on the CIRPAS Twin Otter.

[11] A separate instrument aboard the NOAA P-3 measured CO_2 and CH_4, along with CO and nitrous oxide (N_2O), by quantum cascade laser direct absorption spectroscopy (QCLS) [*Kort et al.*, 2011]. The mean differences between all 10-s averaged QCLS and Picarro CalNex measurements were 0.01 (±0.53) ppmv CO_2 and 4.4 (±3.4) ppbv CH_4. The mean CO_2 differences were larger for flights in which the aircraft cabin temperature approached 40°C; the comparison therefore does not include data from these flights (30 April, 4 May, and 7 May).

2.2. Carbon Monoxide, Black Carbon, Ethane, Propane, and Nitrogen Oxides on the NOAA P-3

[12] CO was measured by vacuum ultraviolet fluorescence spectroscopy [*Holloway et al.*, 2000]. Imprecision of the 1-s CO data is ±1 ppbv; inaccuracy is estimated to be ±5%. During CalNex, the mean difference between all 10-s averaged CO measurements for this and the QCLS instrument was 1.2 (±3.3) ppbv. Black carbon aerosol was measured using a Single Particle Soot Photometer [*Schwarz et al.*, 2008]. Imprecision of the 1-s BC mass mixing ratio data averaged ±20% for the data used here; inaccuracy is estimated to be ±30%. Ethane and propane were measured from whole air samples (WAS) [*Colman et al.*, 2001]. For both measurements, the detection level is 3 pptv and imprecision is ±2%; inaccuracy is estimated to be ±10%. Nitric oxide (NO) was measured by ozone-induced chemiluminescence (CL) [*Ryerson et al.*, 2000]. Imprecision of the NO measurement is ±0.01 ppbv for the 1-s data used here; inaccuracy is estimated to be ±3%. Nitrogen dioxide (NO_2) was measured by photolysis-CL [*Pollack et al.*, 2010]. Imprecision of the NO_2 measurement is ±0.03 ppbv for the 1-s data used here; inaccuracy is estimated to be ±4%. All data reported are 1-s, except for comparisons with WAS, in which 1-s data were averaged over the sample fill time (typically 4–10 s).

2.3. Acetaldehyde on the CIRPAS Twin Otter

[13] Acetaldehyde was measured by proton transfer reaction mass spectrometry (PTRMS) for 100 ms approximately every 0.8 s. Imprecision of the 10-Hz acetaldehyde data is ±0.27 ppbv; inaccuracy is estimated to be ±15% [*Karl et al.*, 2007].

3. Experiment

[14] The NOAA P-3 twice flew over the rice-growing region of the Sacramento Valley (Figure 2) in order to assess changing CH_4 emissions from rice paddies. The first flight on 11 May 2010 occurred just prior to the growing season while many fields were being flooded; the second flight on 14 June 2010 took place early in the growing season. The map in Figure 2a shows the distribution of potential sources of CH_4 in this region, including rice paddies, natural gas wells, dairies [*Salas et al.*, 2008], wetlands, point sources, known biomass burning events, and urban areas in the Sacramento Valley. The rice and wetland data are from the United States Department of Agriculture - National Agricultural Statistics Service (http://nassgeodata.gmu.edu/CropScape/).

[15] The rice paddy studied by *McMillan et al.* [2007] (yellow square, Figure 2a) was planted in mid- to late-May in 2001–2002, approximately one week after flooding. We assume rice farmers throughout the Sacramento Valley followed a similar schedule in 2010–2011, which is qualitatively confirmed by examination of Aeronet MODIS Rapid Response satellite images (NASA/GSFC, Rapid Response, Terra Bands 7-2-1, http://lance-modis.eosdis.nasa.gov/imagery/subsets/?subset=AERONET_Fresno). The 11 May 2010 Aeronet MODIS image (Figure 2b) shows relatively few flooded paddies (black) compared to the image from 29 May, which shows more extensive flooding of the rice paddies (Figure 2c). The Aeronet MODIS image from 14 June shows the paddies turning green as rice shoots appear above the water surface of the flooded paddies (Figure 2d).

3.1. Flight Before Rice Growing Season

[16] On 11 May, the winds in the Sacramento Valley were predominantly from the northwest. The NOAA P-3 entered the northern Sacramento Valley at approximately 11:45 A.M. (all times given in Pacific Standard Time, PST) and flew crosswind transects successively downwind, from northwest to southeast, with periodic vertical profiles. A map of the flight track, colored and sized by CH_4 mixing ratio when in the Sacramento Valley planetary boundary layer (PBL), is provided in Figure 3a. The P-3 flew over Sacramento at 3 P.M. and proceeded to fly crosswind transects down the Sacramento-San Joaquin River Delta before exiting the boundary layer near San Francisco at 3:50 P.M. PST.

3.2. Flights During Rice Growing Season

[17] On 14 June, the NOAA P-3 aircraft flew a similar pattern as before, entered the Sacramento Valley at approximately 12:15 P.M. PST, passed over Sacramento at 3 P.M., and exited the boundary layer near San Francisco at 3:45 P.M. A map of this flight track, colored and sized by CH_4 mixing ratio when in the Sacramento Valley PBL, is provided in Figure 3b. The color and size scales are the same for Figures 3a and 3b. On this day, winds in the Sacramento Valley were predominantly from the southeast, while winds in the Sacramento-San Joaquin River Delta region were predominantly from the west-southwest.

[18] On 15 June 2011, the CIRPAS Twin Otter flight plan focused on the western coastal mountain ranges between Monterey and Mendocino, California. However, the aircraft briefly descended into an area downwind of a rice growing region in the Sacramento Valley, southeast of Arbuckle, California. The wind direction on this day was from the northwest. Examination of the Aeronet MODIS image from this day shows evidence of green rice shoots above the surface of rice paddies, which indicates that this day was also in the rice growing season. Data from this flight segment, the thick orange line in Figure 2a, are discussed in section 4.3.

4. Discussion

[19] In the following sections, we consider different potential sources for CH_4 found in the Sacramento Valley. We extract the contributions from fresh biomass burning emissions from the CH_4 enhancements observed, and define an urban contribution to the remaining enhancements. We then examine CH_4 and CO_2 fluxes from a region with minimal interference from these other potential sources. Finally, we reincorporate all the data from the Sacramento Valley PBL into a mixing model to calculate the estimated contribution of rice cultivation to the CH_4 and CO_2 measured in the entire region.

4.1. Biomass Burning

[20] Biomass burning is a known source of CH_4, CO, and CO_2 to the atmosphere [*Andreae and Merlet*, 2001]. The NOAA P-3 encountered several small biomass burning events on 14 June 2010. The largest was a prescribed burn of grass/wetland in the Sacramento National Wildlife Refuge (SNWR) (see Figure 2a, the light blue patch to the north of the *McMillan et al.* [2007] study site with the filled black circle). Because this burn was located in an area surrounded by wetlands and rice paddies, it is difficult to determine whether the CH_4 measured in the plume came from the combustion process or from the surrounding air entrained into the fire plume. We assume that CH_4 mixing ratios are highest near the surface of the rice paddy, and it is this air that is most likely entrained into the fire. A buoyant combustion plume would loft air with higher levels of CH_4 directly to altitudes observable by the NOAA P-3. Therefore, we cannot assume that all CH_4 enhancements measured in these biomass burning plumes were a direct result of the combustion process.

[21] A time series of CH_4 measured during a spiral descent into the SNWR biomass burning plume is shown in Figure 4. BC increased by 5000 ng/kg, CO increased by 1000 ppbv, and CO_2 increased by 15 ppmv in this plume. CH_4 increased by 100 ppbv, which was about twice the variability in CH_4 outside the plume. This variability contributes to the low correlation between CH_4 and CO in this plume ($r^2 = 0.02$), and complicates comparisons to emission factors. For example, the Environmental Protection Agency (EPA) AP-42 emission factor for the open burning of unspecified weeds is 0.062 mol CH_4/mol CO [*U.S. Environmental Protection Agency*, 1995, chapter 2]. Assuming background levels of 1875 ppbv for CH_4 and 150 ppbv for CO, CH_4 from

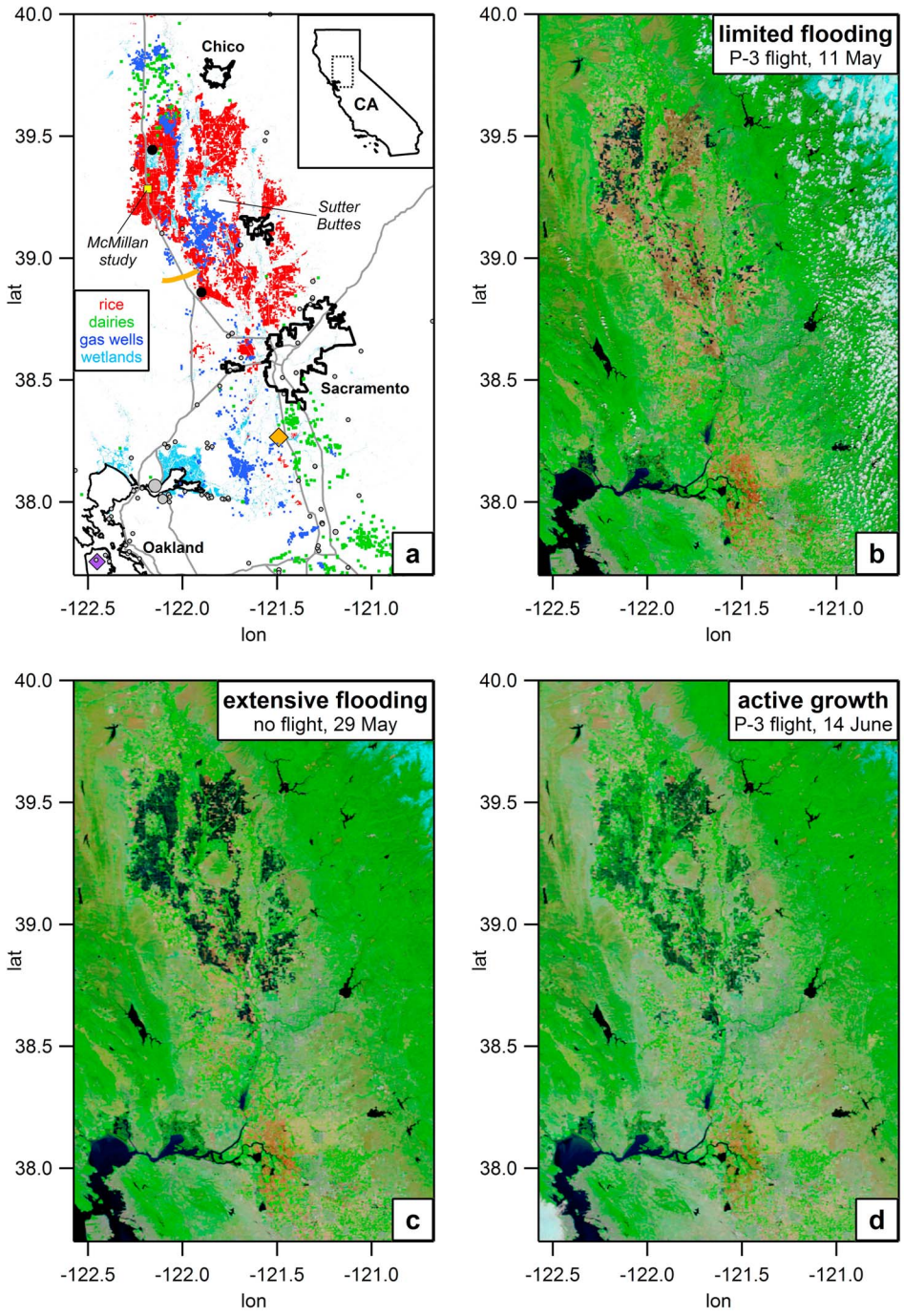

Figure 2. (a) Map of region of study, including possible CH_4 sources in the Sacramento Valley: rice paddies (red); active natural gas wells (blue dots); dairies (green dots); wetlands (light blue); CH_4 point sources (filled gray circles sized by CH_4 emissions), of which the two largest are the Shell Oil Company and Valero refineries, located along the Carquinez Strait; two biomass burning locations on 14 June 2010 (filled black circles); interstate highways (gray lines); and urban areas (outlined by black). The paddy studied by *McMillan et al.* [2007] is located at the yellow square. The Walnut Grove tower is located at the orange diamond; the Sutro tower is located at the purple diamond on the San Francisco Peninsula. The descent into the Sacramento Valley by the CIRPAS Twin Otter is shown with a thick orange line. (b–d) Aeronet MODIS Terra 7-2-1 images on three days in 2010. Figure 2b is the image from 11 May, when few paddies were flooded, assumed to be before the growing season for the majority of rice paddies. Figure 2c shows 29 May; although there was no P-3 flight, the image shows that by this day, nearly all of the rice paddies had been flooded. The black, flooded rice paddies are nearly identical to the red trace in Figure 2a. Figure 2d shows 14 June; by this day, most paddies should have been planted, and the green shoots of rice plants can be seen above the surface of the water in many paddies.

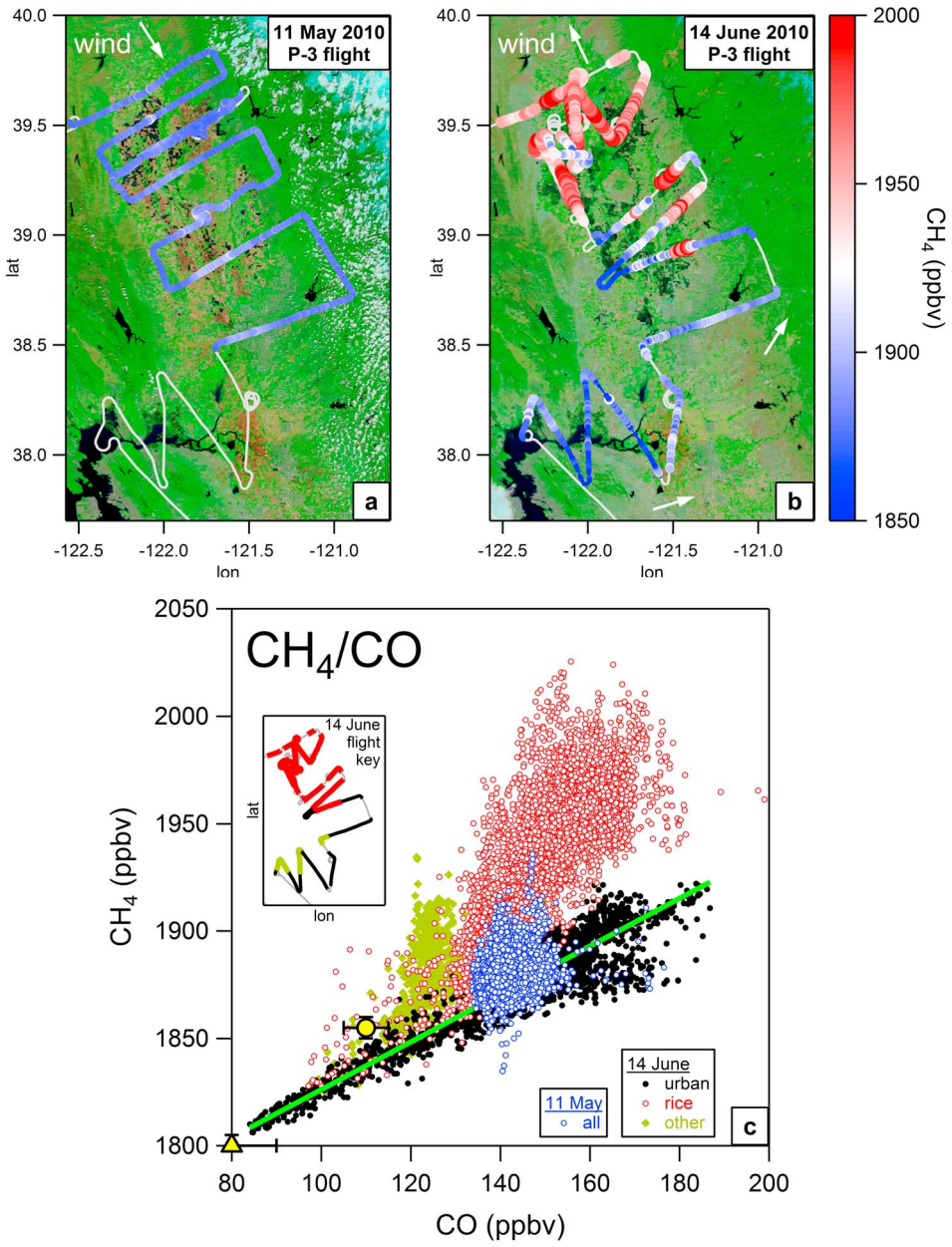

Figure 3. (a) Aeronet MODIS image from 11 May 2010 with prevailing wind direction shown by white arrow, and the P-3 flight track shown in light gray. Measurements of CH_4 in the planetary boundary layer of the Sacramento Valley are colored according to the legend at right. (b) As in Figure 3a, but for 14 June 2010; wind directions varied during the flight and are given by the three white arrows. CH_4 data through the Sacramento-San Joaquin River Delta are included to determine the influence of upwind CH_4 sources on the Sacramento Valley. (c) CH_4 data from Figures 3a and 3b are plotted against measured CO. For 11 May (blue circles), no clear correlation exists between CH_4 and CO, and 1-σ variability in CH_4 is $\pm$8 ppbv, which we attribute to the other CH_4 sources in the area (Figure 2a). For 14 June, a significant enhancement in CH_4 occurs over and downwind of the rice paddies (open red circles) compared to upwind regions on this day and to the 11 May flight. Using location and enhancement ratios with CO, we separate the urban CH_4 emission (filled black circles), located along and to the south of the Sacramento-San Joaquin River Delta and over Sacramento, from other CH_4 emissions (filled olive green diamonds), located to the north of the delta where wetlands predominate (Figure 2a). The map inset in Figure 3c shows the location of these measurements along the 14 June flight track using the same color scheme. The slope of a weighted ODR fit to the urban CH_4/CO enhancement (green line) is 1.11 ($\pm$0.06) ppb CH_4/ppb CO. Also shown are the approximate background levels of CH_4 and CO measured at NOAA ESRL GMD baseline observatories Mauna Loa (yellow triangle) and along the coast of California at Trinidad Head (yellow circle). The error bars for the GMD markers represent the approximate 1-σ seasonal variability.

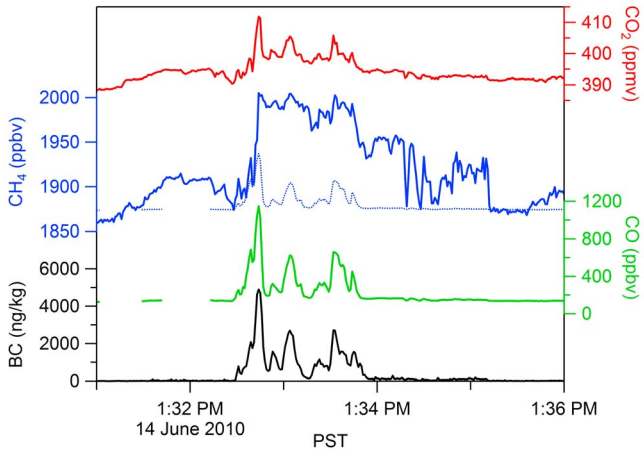

Figure 4. Time series of CO_2 (red), CH_4 (blue), CO (green), and BC (black) during spiral descent into SNWR biomass burning plume. The plume transect resulted in enhancements of up to 1000 ppbv in CO, up to 5000 ng/kg in BC, and 15 ppmv in CO_2. The enhancement in CH_4 based on CO and an AP-42 emission factor for unspecified weeds would appear as the dotted blue trace on the CH_4 axis.

the biomass burning would appear as the dotted blue trace in Figure 4. Assuming this emission factor were correct, this emission would be hidden by the surrounding CH_4 variability. Other biomass burning plumes encountered during this flight resulted in BC enhancements of 1000–2000 ng/kg, CO enhancements of 50–200 ppbv, and CO_2 enhancements of up to 5 ppmv, but any CH_4 enhancement in these plumes was poorly correlated and likely masked by the variability of the surrounding air, as in Figure 4. Outside of these biomass burning plumes, BC and CO vary at most by 500 ng/kg and 100 ppbv, respectively. Scaling from the largest burning plume, we conclude that biomass burning had a small impact ($\ll$20 ppbv) on the CH_4 mixing ratios outside of the freshest biomass burning plumes in the Sacramento Valley on this day.

[22] However, because the biomass burning plumes encountered by the aircraft show significant enhancements in CO and CO_2, we exclude data from plumes with BC enhancements greater than 500 ng/kg for the correlation plots of CH_4/CO and CH_4/CO_2 below, which removes the freshest plumes from these plots. It does not, however, remove any diluted CO and CO_2 biomass burning emissions, which are a source of possible interference in the analysis presented below. For example, as these biomass burning emissions traveled downwind, they may have mixed with CH_4 emissions from the rice paddies. Therefore, after mixing, it would appear that CH_4 and CO were positively correlated. Further, if the CO_2 emissions from biomass burning were greater than the uptake by rice paddies, CH_4 from rice may appear to be positively correlated with CO_2. Ultimately, however, all biomass burning data are used as inputs to the mixing model described later.

4.2. Urban Emissions

[23] On 14 June 2010, southeasterly winds brought urban emissions from Sacramento and the Sacramento-San Joaquin Delta region into the Sacramento Valley. In order to define this urban emission signature, we examine correlations of CH_4 with CO for both flights.

4.2.1. CH_4/CO Before Rice Growing Season

[24] The 11 May CH_4 data shown in Figure 3a are plotted against CO in Figure 3c (blue circles). With relatively clean background air coming from the northwest (Redding, the largest California city north of 40°N latitude, is approximately 100 km upwind of the northernmost NOAA P-3 transect), the CH_4 mixing ratio in the boundary layer averaged 1880 ($\pm$8) ppbv, and was not correlated with CO. We attribute the small residual variability in CH_4 to the other non-rice CH_4 sources in the region, including dairies, natural gas production, and wetlands along the Sacramento River and its tributaries (see Figure 2a). The P-3 did not sample any large sources of CO during this part of the flight.

4.2.2. CH_4/CO During Rice Growing Season

[25] CH_4 mixing ratios measured from the aircraft showed greater variability and were substantially enhanced on 14 June compared to 11 May (Figure 3). Mixing ratios of CH_4 greater than 1950 ppbv were observed over and downwind of rice paddies, which we attribute to rice paddy emissions. The potential sources of CH_4 in the Sacramento Valley other than rice paddies are assumed to have been similar in magnitude on both flight days, although the air temperature in the boundary layer did increase from 14°C on 11 May to 26°C on 14 June. This assumption is based on the three following reasons. First, CH_4 emissions from wetlands and rice scale with biomass [*Whiting and Chanton*, 1993; *McMillan et al.*, 2007], and because wetlands in the Sacramento Valley were green in satellite images both before and during the rice growing season (Figure 2), and they account for only 15% of modeled CH_4 emissions from the Sacramento Valley [*Jeong et al.*, 2012], we conclude that wetlands accounted for less than 15% of possible CH_4 enhancements. Second, ethane and propane correlated better with CO than with CH_4 for both flights. Since ethane and propane are significant natural gas components, this provides evidence that natural gas production in the Sacramento Valley did not account for the increase in CH_4 mixing ratios. Further, the correlations appear to be due to industrial and urban sources from along the Sacramento-San Joaquin River Delta; over the rice growing region of the Sacramento Valley, CH_4 is not well correlated with either ethane or propane (r^2 = 0.32 and 0.13, respectively). Third, according to the CARB greenhouse gas inventory, CH_4 emissions from manure management are not dependent on temperature. We therefore estimate the uncertainty in attributing the CH_4 increase solely to rice cultivation at less than 15%.

[26] As stated above, an additional factor complicates the analysis of the 14 June data: the winds on this day were from the southeast, which brought urban emissions of CO and CH_4 into the Sacramento Valley. This urban CH_4/CO emission signature is apparent upwind of the rice-growing region (Figure 3c). We define an urban CH_4 emission enhancement based on location of sampling and correlations with CO, which are plotted as black filled circles, and sampled from the parts of the flight path along and to the south of the Sacramento-San Joaquin River Delta and over Sacramento (Figure 3c, inset). The remaining data points, sampled from regions to the north of the Delta and plotted as filled olive green diamonds in Figure 3c, show a different correlation with CO than the urban emissions, and are possibly influenced by wetlands north of the San Francisco Bay and the Sacramento-San Joaquin River Delta (see Figure 2a).

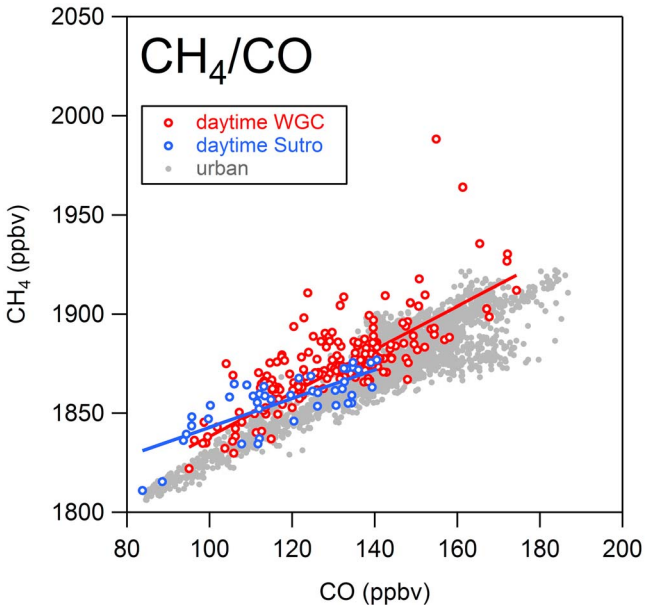

Figure 5. Data for the months of May and June, 2010, between 12 P.M. and 4 P.M. PST from the Walnut Grove tower (WGC), located at the orange diamond in Figure 2a, are plotted as red circles. Data from this same time period from the Sutro tower in San Francisco, located at the purple diamond in Figure 2a, are plotted as blue circles. Weighted ODR fits to these data sets result in CH_4/CO slopes of 1.09 (±0.04) mol/mol at WGC, and 0.72 (±0.10) mol/mol at Sutro tower. Data from urban emissions in Figure 3 are plotted in gray for reference.

[27] Also plotted in Figure 3c are CH_4 and CO mixing ratios, with estimated 1-σ error bars accounting for seasonal variability, measured at the NOAA ESRL GMD Mauna Loa, Hawaii (yellow triangle) and Trinidad Head, California (yellow circle) baseline monitoring observatories for early June, 2010. On 14 June 2010, it appears an air mass more typical of the average Mauna Loa background values in early June influenced the Sacramento-San Joaquin River Delta. We interpret the enhancement ratio in CH_4/CO as urban emissions into this background air mass, because the observed mixing ratios and enhancements are less consistent with the typical Trinidad Head background for early June.

[28] From the defined urban emissions, we attribute CH_4 measurements of greater than 1950 ppbv to strong contributions from rice cultivation emissions. This was the approximate maximum CH_4 mixing ratio measured in air upwind of the rice growing region, from either urban or unknown sources.

4.2.3. Quantifying Urban and Sacramento-San Joaquin Delta Emissions

[29] A linear orthogonal distance regression (ODR) [*Boggs et al.*, 1989] fit to the urban enhancement, weighted by the imprecision of each measurement (weighted ODR), resulted in a slope of 1.11 (±0.06) ppbv CH_4/ppbv CO and is plotted as a green line (Figure 3c). This slope is similar to the daytime enhancement ratio measured from the Walnut Grove tower (38.2650°N latitude, 121.4911°W longitude, orange diamond in Figure 2a) in a collaboration between the California Greenhouse Gases Emission Measurement (CALGEM) project [*Zhao et al.*, 2009] and the NOAA ESRL Tall Tower network (A. E. Andrews et al., Carbon dioxide and carbon monoxide dry air mole fractions from the NOAA ESRL Tall Tower Network, 1992–2009, 2009, ftp://ftp.cmdl.noaa.gov/ccg/towers/). Figure 5 shows all hourly averaged CH_4 and CO data (red circles) sampled from the 483-m above ground level (AGL) Walnut Grove tower inlet between 12 P.M. and 4 P.M. PST for the months of May and June, 2010 (n = 183). A weighted ODR fit to these data resulted in a slope of 1.09 (±0.04) mol CH_4/mol CO. The data identified with an urban signature defined in Figure 3 are plotted as gray circles in Figure 5 for comparison.

[30] Also plotted in Figure 5 (blue circles) are data from afternoon measurements (n = 43) between 12 May and 30 June 2010, at 232 m AGL on a communications tower located on Mt. Sutro (37.7553°N latitude, 122.4517°W longitude, purple diamond in Figure 2a) in San Francisco, California. These tower measurements are also operated by the CALGEM project in collaboration with the NOAA ESRL Tall Tower network. Flask samples at this site were typically taken twice per day: once at night, and once at approximately 2 P.M. PST. A weighted ODR fit to the daytime Sutro tower data resulted in a slope of 0.72 (±0.10) mol CH_4/mol CO. With typical daytime winds in the Sacramento-San Joaquin Delta from the west [*Bao et al.*, 2008], the CH_4/CO emissions ratio increases from west to east from the Sutro tower to the Walnut Grove tower. This increase in CH_4 emissions relative to CO is likely in part due to the wetlands and refineries located along the Sacramento-San Joaquin Delta (which likely account for the CH_4 emissions not correlated with CO, labeled "other," in Figure 3c), including the two largest inventoried CH_4 point sources in California (https://ghgreport.arb.ca.gov/eats/carb/index.cfm), the Shell Oil and Valero refineries, which are the largest two gray circles shown in Figure 2a. Using the data from the Sutro and Walnut Grove towers, we conclude that the urban emissions that influenced the air in the Sacramento Valley on 14 June 2010 were typical of this area during May and June, 2010.

4.3. Rice Paddy Emissions

[31] As stated above, in addition to CH_4 and CO, biomass burning and urban emissions also contain CO_2, which complicates CH_4/CO_2 emission ratio calculations for the rice paddies. In the Sacramento Valley, the urban areas are located along the eastern side, while the two largest known biomass burning events on 14 June 14 2010 were along the western side of the valley (Figure 2a). Therefore, we closely examine one portion of the flight track in the middle of the valley that was over or downwind of rice paddies, but not immediately downwind of urban areas or known biomass burning, in order to discern the clearest signal of rice paddy CH_4 emissions and CO_2 uptake on this day (Figure 6).

[32] The NOAA P-3 flew three vertically stacked north-south transects immediately downwind of several rice paddies that were among the earliest flooded in the 2010 season (Figures 6a–6d). Portions of these transects were selected by latitude (between 39.47°N and 39.565°N latitude) because Aeronet MODIS images show several rice paddies immediately upwind had been flooded by 2 May (Figure 6c) and had started to turn green by 29 May (Figure 6d). The northern latitude limit is upwind of nearby

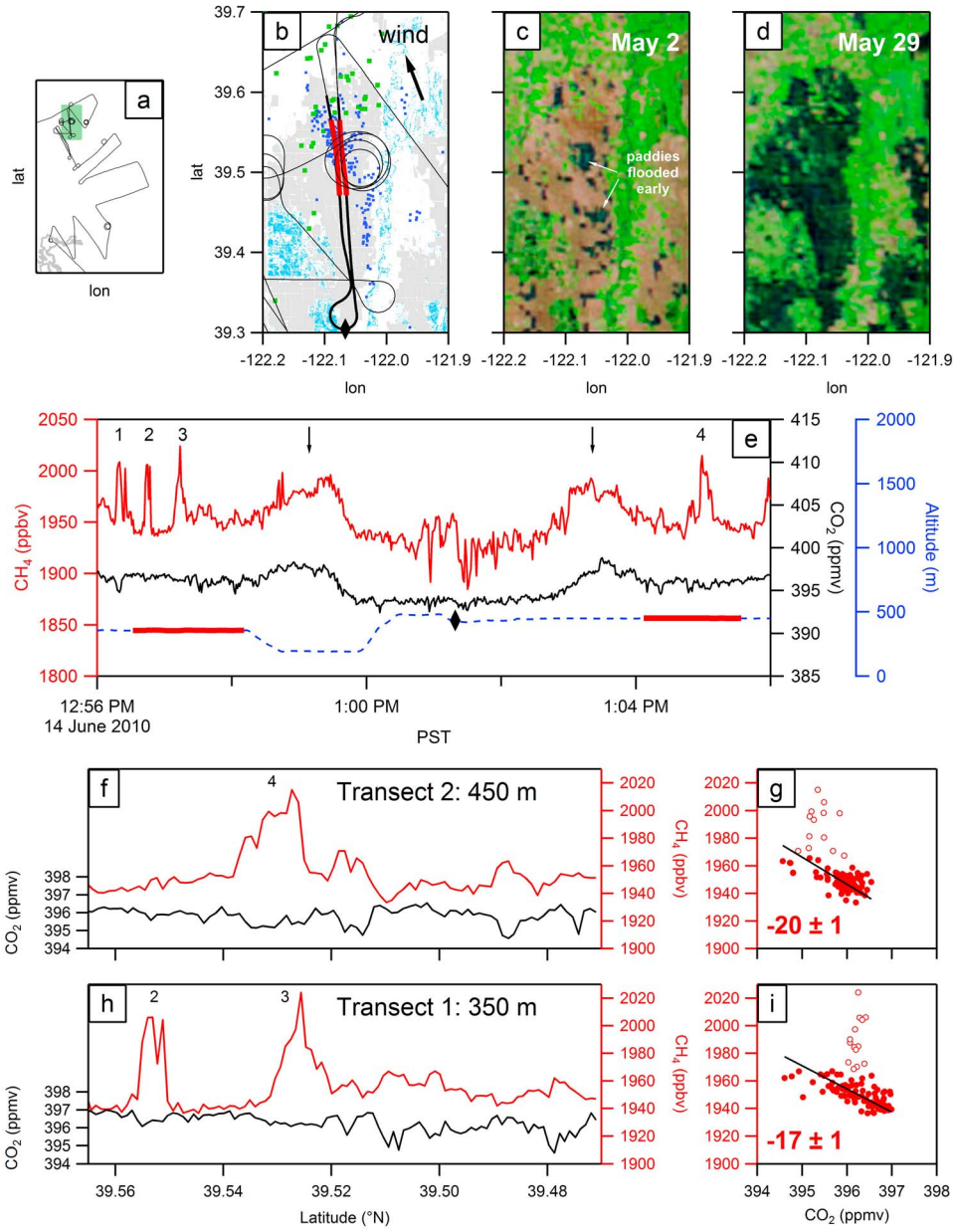

Figure 6. (a) Inset of California from Figure 2 showing 14 June 2010 flight track (black trace) and inset (green rectangle) for Figures 6b–6d. (b) Portion of flight track (black line) over rice paddies (gray). As in Figure 2b, dairies are plotted as green dots, active natural gas wells are plotted as dark blue dots, and wetlands regions are light blue. The left red trace shows a level flight leg at approximately 350 m altitude. The right red trace shows a level flight leg at approximately 450 m altitude. The thin black line is the entire flight track; the thick black line is the portion of the flight track shown in Figure 6e. (c) Aeronet MODIS image from 2 May 2010 showing some of the earlier flooded paddies. (d) Aeronet MODIS image from 29 May 2010 showing these paddies were also among the first to turn green. The red portions of the flight track in Figure 6b are downwind of these paddies. (e) Time series of CH_4 (red), CO_2 (black), and aircraft altitude (dashed blue). The red portions of the altitude trace correspond in time to the latitude-longitude coordinates in Figure 6b. (f) Time series of portion of flight track at the 450-m leg in Figures 6b and 6e. (g) Scatterplot of CH_4 versus CO_2 at the 450-m leg in Figures 6b and 6e. The open red circles represent data with CH_4 > 1970 ppbv. (h) As in Figure 6f, but for the 350-m leg in Figures 6b and 6e. The CH_4 enhancements in Figures 6f and 6h have different CH_4/CO_2 correlation fit slopes to each other and the surrounding air. (i) As in Figure 6g, but for the 350-m leg.

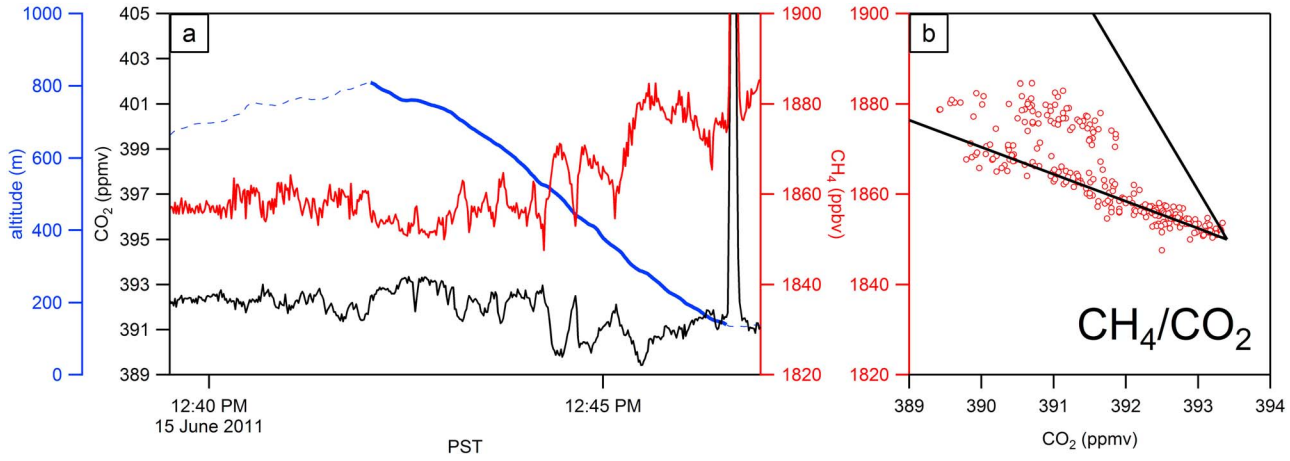

Figure 7. (a) Timeline of CIRPAS Twin Otter descent into Sacramento Valley on 15 June 2011. The top of the descent down to 138 m is plotted as a thick blue line atop the dashed blue altitude trace. (b) Scatterplot of CH_4 versus CO_2 for the descent. The black lines represent the mol/mol flux ratios reported by *McMillan et al.* [2007] for the seedling (−0.6%, lower bound) and mid-vegetative (−2.7%, upper bound) stages of rice growth, with an arbitrary background.

dairies (green dots in Figure 6b). The portion from the lowest altitude transect, flown at approximately 350 m AGL, is denoted by the left red trace in Figure 6b; the portion from the following transect, flown at approximately 450 m AGL, is denoted by the right red trace in Figure 6b. The portion from the highest transect, flown at approximately 575 m AGL, resulted in no correlation between CH_4 and CO_2 ($r^2 = 0.02$), and is therefore not shown in detail. We attribute this lack of correlation to the altitude of the transect; the vertical mixing of this plume had not reached 575 m AGL.

[33] Figure 6e shows a time series of CO_2 and CH_4 data from the portion along the flight track shown as a thick black trace in Figure 6b. The black diamond in Figure 6e shows the same point in time along the flight track in Figure 6b. The red portions of the flight track in Figure 6b are also represented by the red traces in Figure 6e atop the altitude trace.

[34] The lowest two transects showed anti-correlation between CH_4 and CO_2, especially outside the larger plumes of CH_4 (i.e., where CH_4 < 1970 ppbv). The larger CH_4 enhancements, shown in more detail in Figures 6f and 6h, had different correlations with CO_2 (open circles in Figures 6g and 6i), possibly because they were lofted by a combustion process, or because of a greater CH_4 emission per mole of CO_2 taken up by the growing rice. The plumes labeled 1 and 2 in Figure 6e were correlated with enhancements of up to 0.7 ppbv of NO_x (=NO + NO_2), which is emitted primarily from combustion sources. Plume 2 also had an enhancement in CO of 10 ppbv. However, no significant enhancements in NO_x or CO were measured in Plumes 3 or 4.

[35] For data with less than 1970 ppbv CH_4, weighted ODR fits from the 350-m flight leg resulted in a slope of −17 (±1) ppbv CH_4/ppmv CO_2 ($r^2 = 0.48$), or −1.7% mol/mol, and from the 450-m flight leg resulted in a slope of −20 (±1) ppbv CH_4/ppmv CO_2 ($r^2 = 0.37$), or −2.0% mol/mol. These ratios are within the range of CH_4/CO_2 flux ratios measured by *McMillan et al.* [2007] during the early stages of rice growth (−0.6% to −2.7%). For CH_4 measurements greater than 1970 ppbv, a negative correlation with CO_2 exists, but at higher ratios of CH_4 emission to CO_2 uptake than measured by *McMillan et al.* [2007].

[36] A positive correlation between CH_4 and CO_2 appears in Figure 6e, indicated by arrows. These features, sampled to the south of the red traces in Figure 6b, are not correlated with NO_x or BC, but correlated with CO between the arrows, and are well above background levels of CH_4 and CO_2 found above the PBL. This is possibly a residual signature of CH_4 and CO_2 emissions from Sacramento and/or the rice paddies during the nighttime or early morning hours. A calculation based on average wind speed would place this air mass over the rice paddies just to the north of Sacramento at 8 A.M. This is evidence that on broader time scales, the CH_4/CO_2 analysis is influenced by what could be aged urban or nighttime agricultural emissions. This limits our analysis of CO_2 to the high-frequency variability on top of these lower frequency, positively correlated features.

[37] On 15 June 2011, winds were from the northwest, and the chemically instrumented CIRPAS Twin Otter briefly descended into an area downwind of a rice-growing region of the Sacramento Valley, southeast of Arbuckle, California (thick orange line in Figure 2a). With favorable winds compared to the 14 June 2010 flight, this region was not downwind of any large urban area. However, biomass burning was still a potentially complicating factor. During the descent, CH_4 and CO_2 were anti-correlated within the PBL (Figures 7a and 7b). At the bottom of the descent, the aircraft encountered a plume in which mixing ratios of CO_2, CH_4, and acetaldehyde exceeded 415 ppmv, 2000 ppbv, and 40 ppbv, respectively, which, after examination of onboard video, was visibly identified as a biomass burning plume. The plume was located directly above an irrigation canal, denoted as Main Canal on Colusa County, California maps (http://ca-colusacounty.civicplus.com/DocumentView.aspx?DID=543). This was the same irrigation canal along which burning took place on the 14 June 2010 NOAA P-3 flight. The width of the plume corresponded spatially to approximately the width of the canal, indicating the Twin Otter

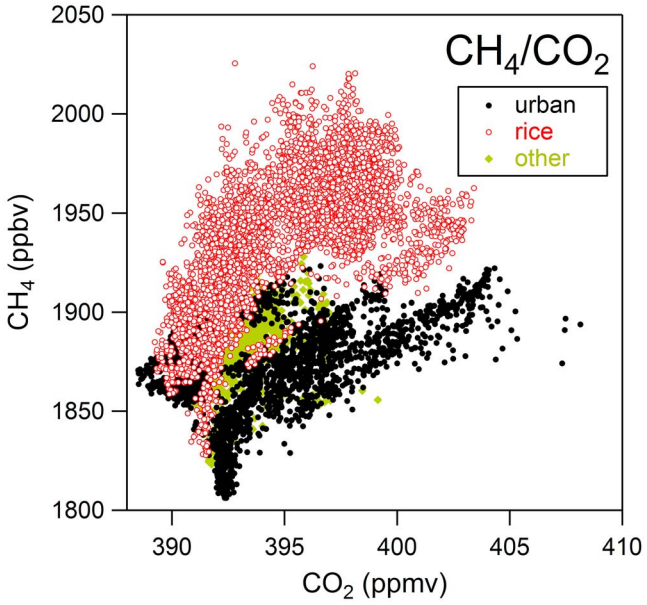

Figure 8. CH_4 versus CO_2 for 14 June 2010, with the same color definitions as Figure 3c. Photosynthetic uptake of CO_2 correlated with CH_4 emissions is difficult to discern within the variability of urban and other CO_2 emissions.

transected the plume before much mixing and broadening of the plume occurred. After encountering this plume, the aircraft turned southeast and flew downwind for several minutes before turning west again and ascending out of the Sacramento Valley. Along this downwind portion of the flight track prior to ascent, the Twin Otter encountered several smaller plumes in which measurements of CH_4, CO_2, and acetaldehyde were positively correlated, which we interpret as influence from biomass burning. Vertical gradients in chemical species measured by PTRMS on the ascent indicate the well-mixed PBL height was approximately 1000 m. Due to the biomass burning plume, we interpret data only from the descent, upwind of most interference from the plume. Figure 7b plots CH_4 versus CO_2 from the top of the descent at 808 m down to 138 m, just before the biomass burning plume. Also plotted are lines representing the expected CH_4/CO_2 flux ratios as reported by *McMillan et al.* [2007] for the seedling and mid-vegetative stages of rice growth. An arbitrary background value was chosen close to the lowest mixing ratios of CH_4 and CO_2 observed during the descent. Data above approximately 300 m fall along the line representing a −0.6% mol/mol flux ratio. Data below this altitude are also negatively correlated and have a similar slope, but with ~10 ppbv more CH_4. We interpret these data as consistent with the flux ratio reported by *McMillan et al.* [2007] for the seedling stage of rice growth.

[38] As stated above, the high frequency anti-correlation of CH_4 and CO_2 is not consistently observed throughout the 14 June 2010 P-3 flight. Using the same urban and rice definitions as in Figure 5, we plot CH_4 versus CO_2 from the 14 June flight in Figure 8. CH_4 and CO_2 are generally positively correlated ($r^2 = 0.41$) above the rice-growing region, likely in part due to biomass burning and urban emissions of CO_2 overwhelming the signal of CO_2 taken up during rice photosynthesis, and in part due to residual, positively correlated emissions of CH_4 and CO_2 from the rice paddies during the night and early morning. According to *McMillan et al.* [2007], during this stage of the growing season, we expect daytime CH_4 emissions to equal approximately 0.6–2.7% of the CO_2 uptake. Given the enhancement of approximately 100 ppbv in CH_4 above the urban emissions in Figure 5, we would expect to see a CO_2 uptake of approximately 4–16 ppmv. However, because the variability of CO_2 from the urban emissions alone spans 15 ppmv, and the diluted emissions from biomass burning add additional CO_2 positively correlated with CH_4 to the area, this rice uptake signal is almost certainly lost in the variability from mixing of other source signatures.

4.4. Mixing Model

[39] Extracting emissions information from observed bivariate relationships (e.g., Figures 3c and 8) is complicated by atmospheric mixing of emissions from multiple sources. We interpret bivariate enhancement ratios as emission ratios only where emission from a single source dominates the relationship (e.g., Figures 6g, 6i, and 7b). Here, we use a multivariate linear regression to derive emission ratios from individual sources based upon the complete data set within the boundary layer in the Sacramento Valley and Sacramento-San Joaquin River Delta from the 14 June 2010 flight (Figures 3c and 8), comprising over 2.5 h of 1-s data (>9000 1-s data points). The multivariate linear regression is formulated as a mixing model [*Nowak et al.*, 2004], which here assumes each 1-s average datum represents a background air parcel with a linear combination of added emissions from urban, biomass burning, and daytime agriculture, each providing enhancements of CH_4, CO_2, CO, and BC with specific and distinct ratios. Initial estimates of enhancement ratios characteristic of each source type are based on measurements made during the flight, and provide initial input to the model. The daytime agricultural CO_2 "emission" is set to be negative, consistent with its uptake in photosynthetic plants. A multivariate, linear least squares fitting routine was applied to all of the data collected in the boundary layer over the Sacramento Valley. In the fit, each measurement is weighted by 1/precision^2, where the precision is the estimated 1-σ variability in a measurement due to variability in the sources' emission of CH_4, CO_2, CO or BC relative to the emissions of the other three or due to other, unaccounted sources of the measured species. The mixing model solves the following system of equations, in the form $\mathbf{Ax} = \mathbf{b}$:

$$\begin{bmatrix} CH_{4_{bkgd}} & CH_{4_{urb}} & CH_{4_{agr}} & CH_{4_{bb}} \\ CO_{2_{bkgd}} & CO_{2_{urb}} & CO_{2_{agr}} & CO_{2_{bb}} \\ CO_{bkgd} & CO_{urb} & CO_{agr} & CO_{bb} \\ BC_{bkgd} & BC_{urb} & BC_{agr} & BC_{bb} \end{bmatrix} \begin{bmatrix} 1 \\ f_{urb\,i} \\ f_{agr\,i} \\ f_{bb\,i} \end{bmatrix} = \begin{bmatrix} CH_{4_i} \\ CO_{2_i} \\ CO_i \\ BC_i \end{bmatrix} \quad (1)$$

where X_i is the mixing ratio for X = CH_4, CO_2, CO, and BC for each *i*th 1-s average datum observed from the P-3 aircraft; *bkgd* represents the assumed background mixing ratio; *urb*, *agr*, and *bb* represent the characteristic relative enhancements in X for urban, daytime agriculture, and biomass burning sources, respectively; and *f* represents the fraction each source contributes to the observed *i*th mixing ratios. The mixing model minimizes the quantity χ^2:

$$\chi^2 = \sum_X \sum_i \left(X_i - \left(f_{urb_i} \times X_{urb} + f_{agr\,i} \times X_{agr} + f_{bbi} \times X_{bb}\right)\right)^2 \times \frac{1}{\sigma_X^2} \quad (2)$$

which is summed over all i data points and over the four gas species, X. The X_{urb}, X_{agr}, and X_{bb} parameters in the matrix **A** of equation (1) are iteratively changed until χ^2 converges to a minimum.

[40] The mixing model achieved a minimum χ^2 with negative correlation between agricultural CH_4 and CO_2 at a slope of -6 (± 2) ppb CH_4/ppm CO_2. Uncertainty on this slope is estimated as the change in the slope of the daytime agriculture air mass that would increase the overall χ^2 by 1, similar to the error estimation set forth by *Bevington* [1969]. The derived uncertainty is robust to the addition in quadrature of a 15% uncertainty due to other CH_4 emission sources in the region. Therefore, this slope is assumed to be the average flux ratio for agricultural emissions in the Sacramento Valley, which is dominated by rice paddies. This slope is consistent with that derived using a bivariate approach in Figure 7b, and is further consistent with the seedling stage of rice growth measured by *McMillan et al.* [2007], which, at the time of the 14 June flight, would include all rice planted after 22 May 2010.

4.5. Comparison of CH_4 Emissions From Rice Cultivation to the CARB Greenhouse Gas Inventory and Recent Studies

[41] The CARB greenhouse gas inventory specifies an annual emission of 122 kg of CH_4 per hectare of rice crop [*Franco*, 2002]. This value was determined by averaging flux results from a variety of farming practices and conditions based on experiments performed in the 1980s and 1990s by *Cicerone et al.* [1992], *Bossio et al.* [1999], *Fitzgerald et al.* [2000], and *Redeker et al.* [2000]. Notably, each of these studies reported at least a factor of 2 increase in CH_4 emissions when rice straw or other organic material was incorporated into the soil before the growing season.

[42] Additionally in the 1990s, with the passage of the Connelly Areias-Chandler Rice Straw Burning Reduction Act of 1991 and Senate Bill 318, the State of California phased down, then banned, most residual rice crop burning in the Sacramento Valley by the year 2001 in an effort to improve air quality in that region. This was significant, because according to the 1990 CARB greenhouse gas inventory (http://www.arb.ca.gov/app/ghg/1990_1990/ghg_sector.php), 99% by area of fields with rice crop residue were burned; in the 2009 inventory, this number had fallen to 11%. This is reflected in the inventory by a decrease in CO_2 emissions from rice crop burning from 1.1 Tg in 1990 to 0.2 Tg in 2009. Presumably, this decrease in burning led to an increase in the incorporation and/or rolling of the rice crop residue into the soil, which, as shown by previous studies, should lead to increased CH_4 emissions in subsequent years. Yet the 122 kg/ha annual CH_4 emission rate has remained unchanged in the CARB greenhouse gas inventory since 1990.

[43] Because only a small percentage of the rice acreage in the Sacramento Valley is burned, the CH_4 fluxes reported by *McMillan et al.* [2007] for a farm that incorporated residual rice crop into the soil are likely representative of the majority of the Sacramento Valley rice crop in the present-day, which is confirmed by our analysis above. For simplicity, we assume the annual CH_4 flux of 348–413 kg/ha reported by *McMillan et al.* [2007] (calculated by 26.1–31.0 g CH_4-C/m^2 $\times$ 16 g CH_4/12 g CH_4-C $\times$ 10^{-3} kg/g $\times$ 10^4 m^2/ha) represents the annual emission rate for the entire Sacramento Valley rice crop. Under this assumption, annual CH_4 emissions from rice cultivation should be increased from 2.7×10^{10} g to 7.8–9.3 $\times$ 10^{10} g in the 2009 inventory, or an increase by a factor of 2.9–3.4, to properly account for changes in rice straw incorporation practices. CH_4 emission from rice cultivation would then represent 5.0–5.8% of inventoried annual California anthropogenic CH_4 emissions.

[44] The CH_4 emissions from rice cultivation in the Sacramento Valley derived here (7.8–9.3 $\times$ 10^{10} g) are also consistent with results from recent studies. *Salas et al.* [2006] estimated CH_4 emissions from rice cultivation in the Sacramento Valley at 6.7×10^{10} g during a warm, dry spring (modeled after the 1997 growing season) and 7.6×10^{10} g during a cool, wet spring (modeled after the 1983 growing season). *Jeong et al.* [2012] reported CH_4 emissions 55 (± 24)% higher than their California-specific inventory, which included the 1983-level CH_4 rice emissions from the study by *Salas et al.* [2006]. *Jeong et al.* [2012] noted a seasonal pattern in modeled CH_4 emissions from the Sacramento Valley, consistent with the rice growing season, and concluded that emissions from rice and wetlands were larger than predicted by *Salas et al.* [2006]. The range of CH_4 emissions derived here are 3–22% greater than the 1983-level emissions estimated by *Salas et al.* [2006], suggesting rice cultivation contributes significantly to the excess CH_4 measured by *Jeong et al.* [2012]. Finally, a parallel work by G. W. Santoni et al. (manuscript in preparation, 2012) uses P-3 data from CalNex and an inverse modeling approach to estimate CH_4 rice emissions in the Sacramento Valley that are consistent with our analysis.

5. Conclusions

[45] Analysis of data from two flights of the NOAA P-3 over the Sacramento Valley shows that during the early stages of the rice growing season, emissions from rice cultivation dominate CH_4 emissions in this region. Spatial coverage provided by the NOAA P-3 complements the temporal coverage of the ground-based study by *McMillan et al.* [2007] in determining flux ratios of CH_4/CO_2 from the rice paddies in this region. Analysis of high-frequency anti-correlation between CH_4 and CO_2 data above one region of the Sacramento Valley found emission fluxes of CH_4 corresponding to between 1.7 and 2.0% of the CO_2 taken up by photosynthesis on a per carbon, or mole to mole, basis for growing rice plants. However, meteorology, biomass burning, and urban emissions of CO and CO_2 complicate this type of analysis. Additional analysis with a mixing model that incorporated these biomass burning and urban emissions resulted in a smaller average agricultural CH_4 flux of 0.6% mol/mol CO_2 taken up, valid for the entire Sacramento Valley on 14 June 2010. Data from one flight of the CIRPAS Twin Otter on 15 June 2011 show a similar flux of CH_4 relative to photosynthetic CO_2 uptake. Our analysis is consistent with fluxes measured during the seedling (0–23 days after planting) and mid-vegetative (24–47 days after planting) stages of rice growth reported by *McMillan et al.* [2007] of 0.6% and 2.7% CH_4/ CO_2 taken up, respectively.

[46] In all, the ratios presented here suggest the findings of *McMillan et al.* [2007] are representative of the entire rice growing region in the Sacramento Valley of California. The annual CH_4 flux reported by *McMillan et al.* [2007] ranges

from 348 to 413 kg/ha, which is approximately three times the CARB greenhouse gas inventory annual emission rate of 122 kg/ha. We attribute this difference to a mandated decrease of rice crop residue burning and the resulting increase in the incorporation and/or rolling of the residue back into the soil, which increases CH_4 emissions the following year by a factor of 2 to 10 [*Cicerone et al.*, 1992; *Bossio et al.*, 1999; *Fitzgerald et al.*, 2000; *Redeker et al.*, 2000]. The emission rate of 122 kg/ha in the CARB inventory was determined from a time when the majority of rice crop residue in California was burned. For simplicity, if we attribute the flux reported by *McMillan et al.* [2007] to the entire California rice crop, then CH_4 emissions from rice cultivation would be a factor of 2.9–3.4 greater than the current CARB greenhouse gas inventory, and would account for 5.0–5.8% of statewide anthropogenic CH_4 emissions.

[47] We note that the increase in CH_4 emissions, which accompanies the decrease in rice crop residue burning, worsens the climate change impact of rice cultivation as predicted by *Cicerone et al.* [1992]. It is an unintended consequence of a policy implemented to improve air quality, and thus provides an example of the difficulties of simultaneously addressing both climate change and air quality through public policy.

[48] **Acknowledgments.** Measurements at Walnut Grove and Mt. Sutro were supported in part by the California Energy Commission (CEC) Public Interest Environmental Research Program and the Director, Office of Science, Office of Basic Energy Sciences, or the U.S. Department of Energy under Contract DE-AC02-05CH11231. Flight time on the CIRPAS Twin Otter was supported by California Air Resources Board contract 09–339 to the University of California, Berkeley.

References

Andreae, M. O., and P. Merlet (2001), Emission of trace gases and aerosols from biomass burning, *Global Biogeochem. Cycles*, *15*(4), 955–966, doi:10.1029/2000GB001382.

Bao, J.-W., S. A. Michelson, P. O. G. Persson, I. V. Djalalova, and J. M. Wilczak (2008), Observed and WRF-simulated low-level winds in a high-ozone episode during the central California ozone study, *J. Appl. Meteorol. Climatol.*, *47*, 2372–2394, doi:10.1175/2008JAMC1822.1.

Bevington, P. R. (1969), *Data Reduction and Error Analysis for the Physical Sciences*, McGraw-Hill, New York.

Boggs, P. T., J. R. Donaldson, R. H. Byrd, and R. B. Schnabel (1989), ODRPACK–Software for weighted orthogonal distance regression, *Trans. Math. Software*, *15*, 348–364, doi:10.1145/76909.76913.

Bossio, D. A., W. R. Horwath, R. G. Mutters, and C. van Kessel (1999), Methane pool and flux dynamics in a rice field following straw incorporation, *Soil Biol. Biochem.*, *31*, 1313–1322, doi:10.1016/S0038-0717(99)00050-4.

Chen, H., et al. (2010), High-accuracy continuous airborne measurements of greenhouse gases (CO_2 and CH_4) using the cavity ring-down spectroscopy (CRDS) technique, *Atmos. Meas. Tech.*, *3*, 375–386, doi:10.5194/amt-3-375-2010.

Cicerone, R. J., and J. D. Shetter (1981), Sources of atmospheric methane: Measurements in rice paddies and a discussion, *J. Geophys. Res.*, *86*(C8), 7203–7209, doi:10.1029/JC086iC08p07203.

Cicerone, R. J., C. C. Delwiche, S. C. Tyler, and P. R. Zimmerman (1992), Methane emissions from California rice paddies with varied treatments, *Global Biogeochem. Cycles*, *6*(3), 233–248, doi:10.1029/92GB01412.

Colman, J. J., A. L. Swanson, S. Meinardi, B. C. Sive, D. R. Blake, and F. S. Rowland (2001), Description of the analysis of a wide range of volatile organic compounds in whole air samples collected during PEM-Tropics A and B, *Anal. Chem.*, *73*(15), 3723–3731, doi:10.1021/ac010027g.

Crosson, E. R. (2008), A cavity ring-down analyzer for measuring atmospheric levels of methane, carbon dioxide, and water vapor, *Appl. Phys. B*, *92*, 403–408, doi:10.1007/s00340-008-3135-y.

Daube, B. C., Jr., K. A. Boering, A. E. Andrews, and S. C. Wofsy (2002), A high-precision fast-response airborne CO_2 analyzer for in situ sampling from the surface to the middle stratosphere, *J. Atmos. Ocean. Technol.*, *19*(10), 1532–1543, doi:10.1175/1520-0426(2002)019<1532:AHPFRA>2.0.CO;2.

Dlugokencky, E. J., R. C. Myers, P. M. Lang, K. A. Masarie, A. M. Crotwell, K. W. Thoning, B. D. Hall, J. W. Elkins, and L. P. Steele (2005), Conversion of NOAA atmospheric dry air CH_4 mole fractions to a gravimetrically prepared standard scale, *J. Geophys. Res.*, *110*, D18306, doi:10.1029/2005JD006035.

Fitzgerald, G. J., K. M. Scow, and J. E. Hill (2000), Fallow season straw and water management effects on methane emissions in California rice, *Global Biogeochem. Cycles*, *14*(3), 767–776, doi:10.1029/2000GB001259.

Franco, G. (2002), Inventory of California greenhouse gas emissions and sinks: 1990–1999, *Rep. 600–02–001F*, Calif. Energy Comm., Sacramento.

Hegg, D. A., D. S. Covert, H. Jonsson, and P. A. Covert (2005), Determination of the transmission efficiency of an aircraft aerosol inlet, *Aerosol Sci. Technol.*, *39*, 966–971, doi:10.1080/02786820500377814.

Holloway, J. S., R. O. Jakoubek, D. D. Parrish, C. Gerbig, A. Volz-Thomas, S. Schmitgen, A. Fried, B. Wert, B. Henry, and J. R. Drummond (2000), Airborne intercomparison of vacuum ultraviolet fluorescence and tunable diode laser absorption measurements of tropospheric carbon monoxide, *J. Geophys. Res.*, *105*(D19), 24,251–24,261, doi:10.1029/2000JD900237.

Jeong, S., C. Zhao, A. E. Andrews, L. Bianco, J. M. Wilczak, and M. L. Fischer (2012), Seasonal variation of CH_4 emissions from central California, *J. Geophys. Res.*, *117*, D11306, doi:10.1029/2011JD016896.

Karl, T., A. Guenther, R. J. Yokelson, J. Greenberg, M. Potosnak, D. R. Blake, and P. Artaxo (2007), The tropical forest and fire emissions experiment: Emission, chemistry, and transport of biogenic volatile organic compounds in the lower atmosphere over Amazonia, *J. Geophys. Res.*, *112*, D18302, doi:10.1029/2007JD008539.

Kort, E. A., P. K. Patra, K. Ishijima, B. C. Daube, R. Jimenez, J. Elkins, D. Hurst, F. L. Moore, C. Sweeney, and S. C. Wofsy (2011), Tropospheric distribution and variability of N_2O: Evidence for strong tropical emissions, *Geophys. Res. Lett.*, *38*, L15806, doi:10.1029/2011GL047612.

Lauren, J. G., G. S. Pettygrove, and J. M. Druxbury (1994), Methane emissions associated with a green manure amendment to flooded rice in California, *Biogeochemistry*, *24*(2), 53–65, doi:10.1007/BF02390179.

Le Mer, J., and P. Roger (2001), Production, oxidation, emission and consumption of methane by soils: A review, *Eur. J. Soil Biol.*, *37*, 25–50, doi:10.1016/S1164-5563(01)01067-6.

McMillan, A. M. S., M. L. Goulden, and S. C. Tyler (2007), Stoichiometry of CH_4 and CO_2 flux in a California rice paddy, *J. Geophys. Res.*, *112*, G01008, doi:10.1029/2006JG000198.

Nowak, J. B., et al. (2004), Gas-phase chemical characteristics of Asian emission plumes observed during ITCT 2K2 over the eastern North Pacific Ocean, *J. Geophys. Res.*, *109*, D23S19, doi:10.1029/2003JD004488.

Peischl, J., et al. (2010), A top-down analysis of emissions from selected Texas power plants during TexAQS 2000 and 2006, *J. Geophys. Res.*, *115*, D16303, doi:10.1029/2009JD013527.

Pollack, I. B., B. M. Lerner, and T. B. Ryerson (2010), Evaluation of ultraviolet light-emitting diodes for detection of atmospheric NO_2 by photolysis-chemiluminescence, *J. Atmos. Chem.*, *65*(2–3), 111–125, doi:10.1007/s10874-011-9184-3.

Redeker, K. R., N.-Y. Wang, J. C. Low, A. McMillan, S. C. Tyler, and R. J. Cicerone (2000), Emissions of methyl halides and methane from rice paddies, *Science*, *290*, 966–969, doi:10.1126/science.290.5493.966.

Ryerson, T. B., E. J. Williams, and F. C. Fehsenfeld (2000), An efficient photolysis system for fast-response NO_2 measurements, *J. Geophys. Res.*, *105*(D21), 26,447–26,461, doi:10.1029/2000JD900389.

Salas, W., P. Green, S. Frolking, C. Li, and S. Boles (2006), Estimating irrigation water use for California agriculture: 1950s to present, *Rep. CEC-500–2006–057*, Public Interest Energy Res. Program, Calif. Energy Comm., Sacramento.

Salas, W., C. Li, F. Mitloehner, and J. Pisano (2008), Developing and applying process-based models for estimating greenhouse gas and air emission from California dairies, *Rep. CEC-500-2008-093*, Public Interest Energy Res. Program, Calif. Energy Comm., Sacramento.

Schwarz, J. P., et al. (2008), Coatings and their enhancement of black carbon light absorption in the tropical atmosphere, *J. Geophys. Res.*, *113*, D03203, doi:10.1029/2007JD009042.

U.S. Environmental Protection Agency (1995), *Compilation of Air Pollutant Emission Factors: Volume 1: Stationary Point and Area Sources*, *Rep. EPA-AP-42*, Off. of Air Quality Plann. and Stand., Research Triangle Park, N. C.

Whiting, G. J., and J. P. Chanton (1993), Primary production control of methane emission from wetlands, *Nature*, *364*, 794–795, doi:10.1038/364794a0.

Zhao, C., A. E. Andrews, L. Bianco, J. Eluszkiewicz, A. Hirsch, C. MacDonald, T. Nehrkorn, and M. L. Fischer (2009), Atmospheric inverse estimates of methane emissions from Central California, *J. Geophys. Res.*, *114*, D16302, doi:10.1029/2008JD011671.

Zhao, C. L., and P. P. Tans (2006), Estimating uncertainty of the WMO mole fraction scale for carbon dioxide in air, *J. Geophys. Res.*, *111*, D08S09, doi:10.1029/2005JD006003.